

# Electronic distortion in keV particle bombardment

Reena Bhatia and Barbara J. Garrison

Department of Chemistry, The Pennsylvania State University, University Park, Pennsylvania 16802

(Received 1 February 1994; accepted 24 February 1994)

The angle resolved velocity distributions of excited ( $^4F_{7/2}$ ) and ground state ( $^4F_{9/2}$ ) Rh atoms ejected from the Rh {100} surface due to keV Ar<sup>+</sup> ion bombardment are described with a model that takes into account the local electronic environment. The lifetime of the excitation probability for each excited Rh atom is assumed to depend on the local embedded-atom method (EAM) density. It is thus possible to distinguish between ejected atoms that experience very little difference in their electronic environments. Although most excited atoms that survive with significantly high excitation probabilities originate from the surface layer, it is not uncommon for an atom beneath the surface to eject from a disrupted environment and end up with a high excitation probability. This model improves upon a previous one, where the lifetime was assumed to vary with the height above the original surface.

## I. INTRODUCTION

The bombardment of solids with keV atoms or ions leads to rather violent collisions with subsequent ejection of target particles. This process results in atoms and molecules, either neutral or charged, in a large variety of internal states which eject into the vacuum. This large manifold of ejection products means that a description of all the microscopic events simultaneously is overly complex. The motion of the nuclei in their ground electronic state can be well described by molecular dynamics simulations.<sup>1,2</sup> These simulations yield microscopic pictures of reaction mechanisms as well as quantities such as energy and angular distributions that can be directly compared to experimental quantities. The situation for describing electronic (excitation, ionization) events in keV particle bombardment, however, is not as mature.

A big challenge for describing electronic events in keV particle bombardment is that the solid is "distorted" from equilibrium when a particle ejects into the vacuum. Moreover, each atom's path is individualistic and thus it experiences its own electronic environment during the course of the atomic motion. The theoretical challenge is to maintain the individual nature of each atomic motion yet to be able to incorporate changes in electronic environment in any proposed model. Most electronic structure techniques, however, are computationally time consuming and thus are prohibitive to perform at every integration step for a multitude of atoms. The general strategies have been either to assume a quiescent band structure<sup>3-9</sup> or to perform electronic structure calculations on small clusters assuming a somewhat limited set of atomic motions.<sup>10-12</sup>

Recently we have been interested in the excitation of atoms into fine-structure states and subsequent deexcitation during the course of a keV particle bombardment event. For example, the energy and angular distributions of Rh atoms ejected from Rh {100} in both the ground,  $^4F_{9/2}$ , and excited,  $^4F_{7/2}$ , fine-structure states have been measured and found to be different from each other.<sup>13,14</sup> A simple model was developed to explain these differences and it was found that col-

lisions in the 1–20 Å range above the surface give rise to an anomalous feature in the plots of the ratio of the excited state intensity to the ground state intensity.<sup>13,14</sup> This model assumes that an atom is excited if it gets within a distance  $r_{th}$  of another atom. The excitation probability decays in time with a lifetime  $\tau$  as the atom moves through the solid and into the vacuum. The lifetime  $\tau$  depends upon the height of the atom above the surface but not upon any possible local disorder of the system.

In this paper we present an extension of this model that takes into account the local electronic environment in the solid. In particular, we have been using the embedded-atom method (EAM) potentials<sup>15-17</sup> in molecular dynamics simulations to describe the interaction among the Rh atoms. One of the parameters of the EAM potential is the local density  $\rho$  at each atom. We now use the local density to determine the lifetime of the decay process. This density provides an interesting indicator of the local electronic environment in the system. In particular, it allows the identification of events for which the local environment is significantly distorted from equilibrium.

## II. DESCRIPTION OF THE MODEL AND CALCULATION

In this section we briefly describe an approach for calculating the velocity- and angle-dependent distributions of Rh atoms ejected in their ground and excited states due to ion bombardment. In simulating the ejection of these species, one must treat both the atomic motions and the electronic excitations. As previously discussed,<sup>1</sup> the molecular dynamics (MD) simulations have been used successfully to describe the velocity- and angle-dependent distributions of the ground state species. The details of the calculations have been described elsewhere.<sup>13,14,18</sup> An EAM potential is used to describe the interatomic interactions. The energy for the  $i$ th atom is given by

$$E_i = F[\rho_i = \sum_{j \neq i} \rho_{\text{atomic}}(r_{ij})] + \frac{1}{2} \sum_{j \neq i} \phi(r_{ij}), \quad (1)$$

where  $r_{ij}$  is the distance between the  $i$ th and  $j$ th atoms. The first term is the embedding function, which is the energy of the interaction of the ion core with the electron sea of density  $\rho_i$ . The second term is short-ranged and is the ion-core repulsion at a distance of separation  $r_{ij}$  of the two cores. The total density  $\rho_i$  is assumed to be a sum of atomic densities,  $\rho_{\text{atomic}}(r_{ij})$ , which depend approximately exponentially on the distance between atoms  $i$  and  $j$ . It is not overly important for the model described below that this density be absolutely correct. Rather, the major feature is that it allows one to distinguish among the electronic environments for different configurations of atoms.

The calculation of the electronic excitations<sup>19,20</sup> employs a method based upon a collisional excitation mechanism. This model is computationally attractive since it requires no explicit electronic structure calculations. It is based on the curve-crossing theory of Fano and Lichten<sup>21</sup> which assumes that colliding atoms are excited (with initial excitation probability  $P_0$ ) when the distance of closest approach drops below some threshold value,  $r_{\text{th}}$ . Once the collision is over, the excitation of atom  $i$  is subjected to the time-dependent decay

$$dP_i/dt = -P_i/\tau_i. \quad (2)$$

The instantaneous excitation probability  $P_i$ , or the probability that the atom  $i$  remains excited at any given time, is evaluated at every time step until the atom ejects into the vacuum. The lifetime  $\tau_i$  is based on some empirically determined, environment-sensitive quantity. It is assumed that relaxation is a result of the coupling between the excited electron and the electrons in the remainder of the solid. In contrast to our previous studies<sup>13,14</sup> where  $\tau_i$  depended only on the height of the atom relative to the initial undisturbed crystal, here we use the density  $\rho_i$  to determine the lifetime as

$$1/\tau_i = c\rho_i, \quad (3)$$

where  $c$  is a constant to be determined and the density  $\rho_i$  is the EAM density. This expression allows  $\tau_i$  to fluctuate about some constant value in the bulk and allows its value to approach infinity when the atom is far from the solid. This latter condition is appropriate since the current studies deal with metastable excited states of Rh atoms. With this parameterization of the excitation model there are three parameters to be determined— $r_{\text{th}}$ ,  $P_0$ , and  $c$ .

It is useful to examine the consequences of this model for a simplistic limiting case. If we assume that the density is a constant out to a distance  $z_{\text{max}}$  above the surface and then falls to zero, that the collision occurs at  $z_{\text{min}}$ , and that the velocity of the atom is constant, we obtain

$$dP/dt = -P/\tau \quad \text{or} \quad dP/P = -dt/\tau \quad (4)$$

$$\text{or} \quad \ln(P/P_0) = -z_{\text{min}} \int_{z_{\text{min}}}^{z_{\text{max}}} c\rho dz/v_{\perp},$$

where we have used the equality  $dt = dz/v_{\perp}$ , with  $v_{\perp}$  being the velocity component perpendicular to the surface. This integrates to

$$P = P_0 \exp[-c\rho(z_{\text{max}} - z_{\text{min}})/v_{\perp}] \quad (5a)$$

$$= P_0 \exp(-A/av_{\perp}), \quad (5b)$$

where  $A$  and  $a$  are the generally used constants in this expression.<sup>22</sup> Equations (5) show that the final excitation probability depends exponentially on the reciprocal of the perpendicular component of the velocity. This has been the conventional expression used for data analysis and has worked reasonably well except for binding energy effects at low velocities.<sup>5,7,11</sup> There is also an implication in Eqs. (5) that the ratio  $A/a$  should depend on the density appropriate for an individual atom's motion as it ejects from the solid. As will be shown later, this can depend on the angles of ejection. It was observed in the experimental data that the best fit values of  $A/a$  depend on the angles of ejection.<sup>13</sup>

The expression in Eq. (5a) for the final excitation probability gives insight into the factors that can cause deviations from Eq. (5b). First, the density is not constant as an atom ejects although one might argue that it is the same for all atoms that eject. Second, there is a dependence of the final excitation probability on  $z_{\text{min}}$ . For a surface atom to be ejected, an atom from beneath must hit it. Since realistic potentials are being used, the collision does not occur instantaneously. As the atom beneath moves toward the surface atom, for some time period both atoms move above the plane ( $z=0$ ) where the surface atom started. They reach a distance of closest approach and then the surface atom ejects. The definition of the time and height when a collision begins is open to discussion but almost any definition will result in a value for the height that depends on the collision velocity. We have chosen to start the time clock for the integration of Eq. (2), and thus the deexcitation process, when the two colliding atoms are moving apart and the distance between them is  $r_{\text{th}}$ .

This model has fewer adjustable parameters than the height model used previously. The value of  $r_{\text{th}}$  was chosen to have the same value of 1.85 Å as used previously.<sup>13,14,18</sup> The values of  $P_0$  and  $c$  are fit to the experimental data for particles that eject within 20° of normal of the surface. The specific values are  $P_0=0.866$  and  $c=5.22/\text{fs}/(e^-/\text{Å}^3)$  where  $\text{fs}=10^{-15}$  s and  $e^-$  is the electron charge. This value of  $c$  means that for an atom in the bulk with an equilibrium density of  $0.03535 e^-/\text{Å}^3$ , the corresponding lifetime is 5.4 fs, and for an atom on the surface with an equilibrium density of  $0.0236 e^-/\text{Å}^3$ , the lifetime is 8 fs. These values are slightly smaller than found previously and actually fit better with accepted lifetimes.<sup>23</sup> In the event of a collision the density values are significantly higher than these equilibrium values and hence, the initial lifetimes are much smaller.

### III. RESULTS

In an attempt to understand the electronic dynamics of the ejection process several workers have tried to select idealized atomic motions that give rise to the ejection of atoms.<sup>4,5,9-12,24</sup> Several such motions in which atom No. 1 ejects are depicted in Fig. 1. In all cases the simulations are three-dimensional, the collisional motions are initiated by giving an atom in the solid an arbitrary velocity in a specified direction and the final (measurable) velocity of the ejected atom perpendicular to the surface is  $5 \times 10^5$  cm/s which corresponds to a perpendicular energy of 13 eV. The motion in Fig. 1(b) has a third layer atom (No. 2) hitting in a head-on

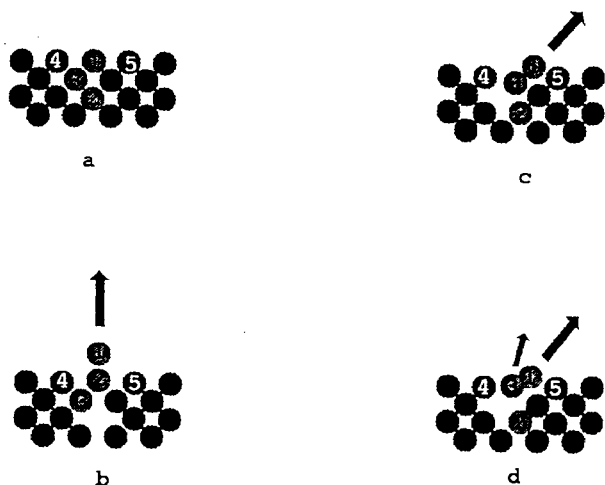


FIG. 1. Pictorial representations of the idealized motions. See the text for a description.

collision atom No. 1 directly above it and ejecting the atom No. 1 normal to the surface ( $\theta = 0^\circ$ ). The motion in Fig. 1(c) has a second layer atom (No. 3) hitting head-on atom No. 1 in the first layer. The initial angle of approach is  $\theta_i = 45^\circ$  but due to the attractive forces of atom No. 1 to the solid, the final angle is  $50^\circ$  with respect to the surface normal. Finally atom No. 3 can also hit atom No. 1 with an initial angle of approach of  $\theta_i = 25^\circ$  or  $30^\circ$ , causing atom No. 1 to move sideways. Atom No. 1 then glances off atom No. 5 and ends up with a final angle of  $50^\circ$ . It should be noted that these idealized cases are ones that we have chosen to illustrate the complexity of even simple collision processes and that there are undoubtedly other idealized motions that could have been chosen.

The results of calculating the excitation probability for these idealized motions are shown in Fig. 2. For the two head-on sequences [Figs. 1(b) and 1(c)] there is a large range of velocities that gives rise to ejection at approximately the same final angle. For incident angles of approach of atom No. 3 of  $25^\circ$  or  $30^\circ$ , there is only a small range of starting conditions that gives rise to ejection at  $50^\circ \pm 5^\circ$ . In the simple expressions of Eq. (5) and that of Hagstrum<sup>22</sup> the final excitation probability depends only on  $v_\perp = v \cos \theta$ , and not independently on either the total velocity  $v$  or the polar angle of ejection  $\theta$ . The first obvious conclusion to draw from Fig. 2 is that the results do depend on more details of the motion than just  $v_\perp$ .

By examination of the two head-on collision sequences, we find from Eq. (5a) that there are three possible reasons for the excitation probability to depend on the specific atomic motions. First, the electron density that the ejecting atom experiences is different for the four cases. Shown in Fig. 3(a) is the density of atom No. 1 as a function of height above the surface for both head-on collision sequences. As shown Figs. 1(b) and 1(c), when atom No. 1 ejects straight-up it leaves a void behind it. When atom No. 1 moves sideways, it has atoms and electrons below it. Consequently, an atom ejecting off-normal undergoes more deexcitation and its excitation

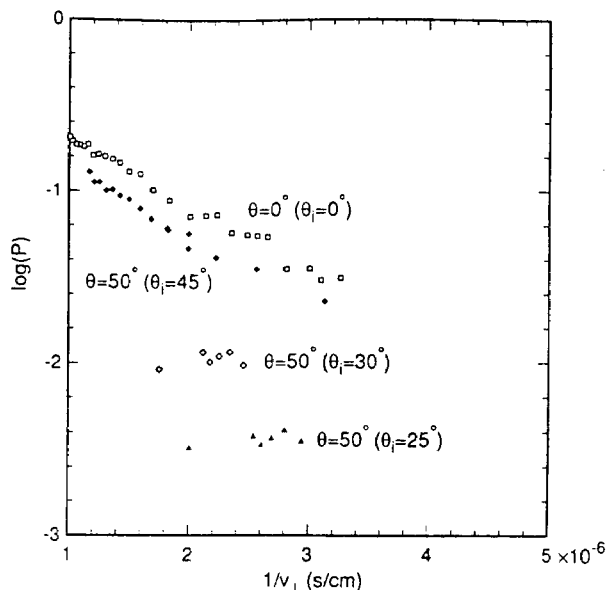


FIG. 2.  $\log(P)$  vs  $1/v_\perp$  for four ideal cases in which the final (i.e., measurable) perpendicular component of velocity is  $5 \times 10^5$  cm/s which corresponds to 13 eV for Rh atoms. The curve labeled  $\theta = 0^\circ$  is for motion shown in Fig. 1(b). The other three curves correspond to motions in which the final (measurable) angle is  $\sim 50^\circ$ . The angle of incidence of the second layer atom is either head-on [ $\theta_i = 45^\circ$ , Fig. 1(c)] or off-center [ $\theta_i \approx 30^\circ, 25^\circ$ , Fig. 1(d)].

probability is lower. Second, as mentioned above, the velocity is not constant in the near surface region. Shown in Fig. 3(b) is the velocity of the atom that ejects at  $\theta = 0^\circ$  as a function of the height above the surface. The velocity maximizes at about  $z = 1$  Å and then decreases slightly because the attractive potential to the surface must be overcome (i.e., the surface binding energy effect).<sup>6,11</sup> The  $v_\perp$  component for the head-on collision sequence for  $\theta_i = 45^\circ$  is similar although the value is slightly larger indicating that the excitation probability for off-normal ejection should be larger for  $\theta_i = 0^\circ$  which is the opposite trend of the computational results in Fig. 2. Finally, as discussed previously<sup>14</sup> the collision which knocks off an atom is not an instantaneous event that occurs at a height of 0 Å. The conclusion that the final excitation probability only depends on  $v_\perp$  is based on an integration over height above the surface with the integral limits of  $(0, \infty)$ .<sup>22</sup> The value of  $z_{\min}$  is 0.3–0.4 Å in both ideal cases. The explanation for the two head-on collision sequences at different final ejection angles is that the difference in density and thus electron density is the dominant effect that causes the excitation probabilities to be different.

The analogous plots of velocity components and density vs height above the surface are shown for the two other idealized collision sequences in Figs. 3(c) and 3(d). For these collision processes, after atom No. 1 is struck by atom No. 3, it moves towards atom No. 5 with a small component of velocity perpendicular to the surface and a large component parallel to the surface. It is deflected and ejects at an angle of  $50^\circ$ . In these cases both the density factor and the velocity factor indicate that the final excitation probability should be lower than for the head-on collision sequences. For all of these ideal cases there is a large contribution from the chang-

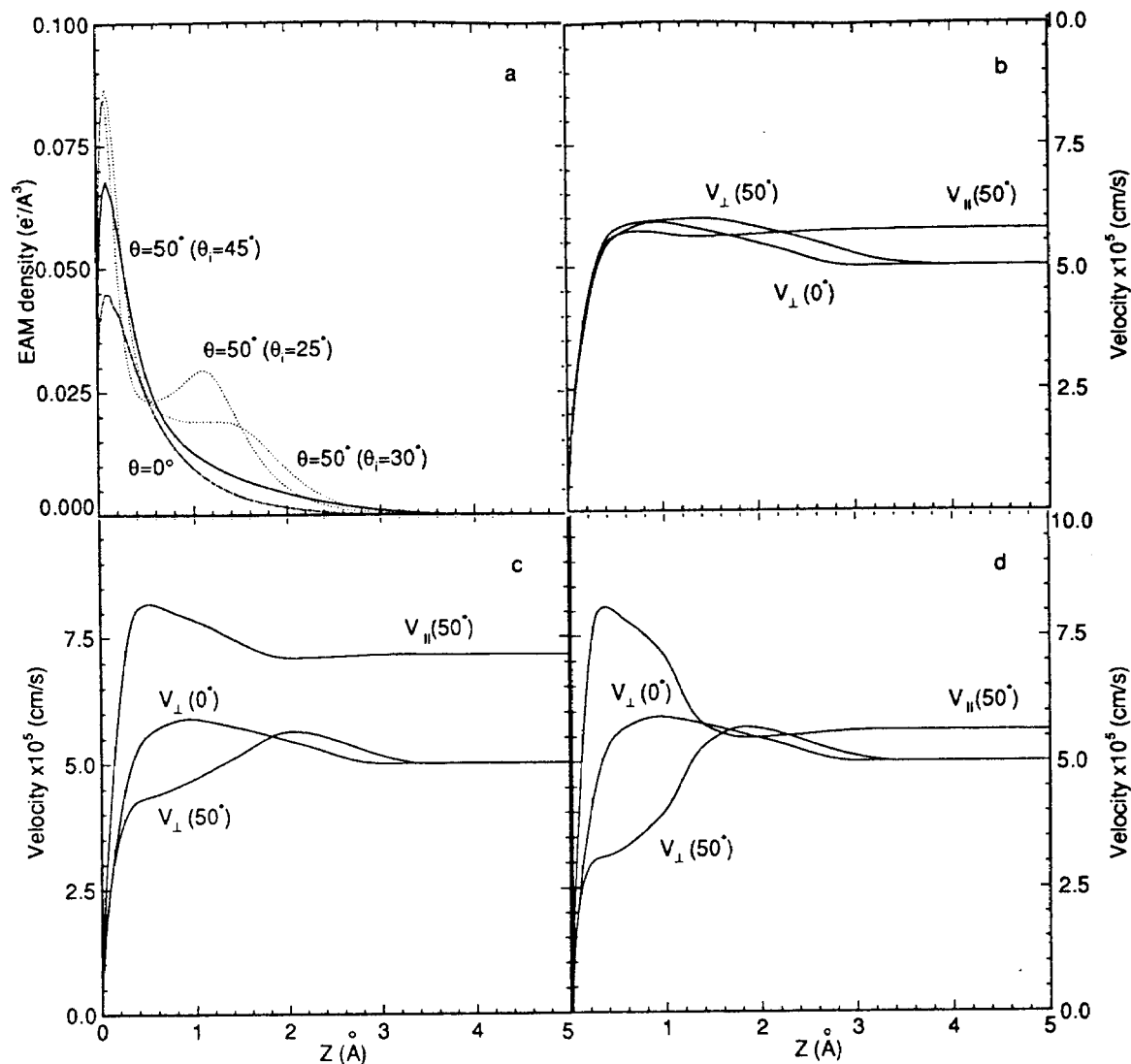


FIG. 3. Collisional details of the four idealized cases of Figs. 1 and 2. (a) Density vs height above the surface  $z$ . (b) Perpendicular and parallel components of velocity for the  $\theta_i=0^\circ$  and  $45^\circ$  head-on cases. (c) Perpendicular and parallel components of velocity for  $\theta_i=30^\circ$  off-center case. The  $\theta_i=0^\circ$  data is repeated for comparison. (d) Perpendicular and parallel components of velocity for  $\theta_i=25^\circ$  off-center case. The  $\theta_i=0^\circ$  data is repeated for comparison. In (b)–(d) the final angle is  $50^\circ$ .

ing density that would not be apparent in models where the lifetime of decay only depends upon the height of the atom above the surface.

Results from the full molecular dynamics simulations are shown in Fig. 4 for three different angle ranges, namely, straight-up ( $\theta \leq 20^\circ$ ), off-normal along the open crystallographic direction ( $30^\circ \leq \theta \leq 50^\circ$ ,  $\varphi \approx 0^\circ$ ), and off-normal along the close-packed crystallographic direction ( $30^\circ \leq \theta \leq 50^\circ$ ,  $\varphi \approx 45^\circ$ ). The average quantities are shown in Fig. 4(a). There are several features worth noting. First, there is more scatter in the points [Figs. 4(b)–(d)] than found for the previous model. Part of the reason for this is that there was an error in the computer code.<sup>25</sup> The more substantive reason, though, is that this density model is more sensitive to the different environments that can exist at the time of collision and during the subsequent motion. The second interesting feature is the broadband of points that encompasses but does not closely follow the ideal case. The results from the height

model followed the ideal case line much more closely.<sup>14</sup> (As an aside, because of the large spread in points, the parameters had to be fit to the actual simulations rather than the ideal case.) The atoms are experiencing a much larger variety of environments than the pristine one of the ideal case. In other words, the ideal case is not always a reasonable representation of the actual scattering events.

Concentrating on the high velocity regime, for ejection normal to the surface there appear to be two bands of points, one below and one above the ideal case line [Fig. 4(b)]. The band above corresponds to atoms that experience a density of  $0.0225 \text{ e}^-/\text{\AA}^3$  or lower at the time of excitation. Typically, these are atoms excited 1–20  $\text{\AA}$  above the surface. For off-normal ejection, there are three bands, one below and two above the ideal case line. The topmost band (density at excitation,  $\rho_i < 0.0225 \text{ e}^-/\text{\AA}^3$ ) corresponds to events where the ejecting atom is first hit such that it starts to move into the vacuum and then undergoes a second collision with a

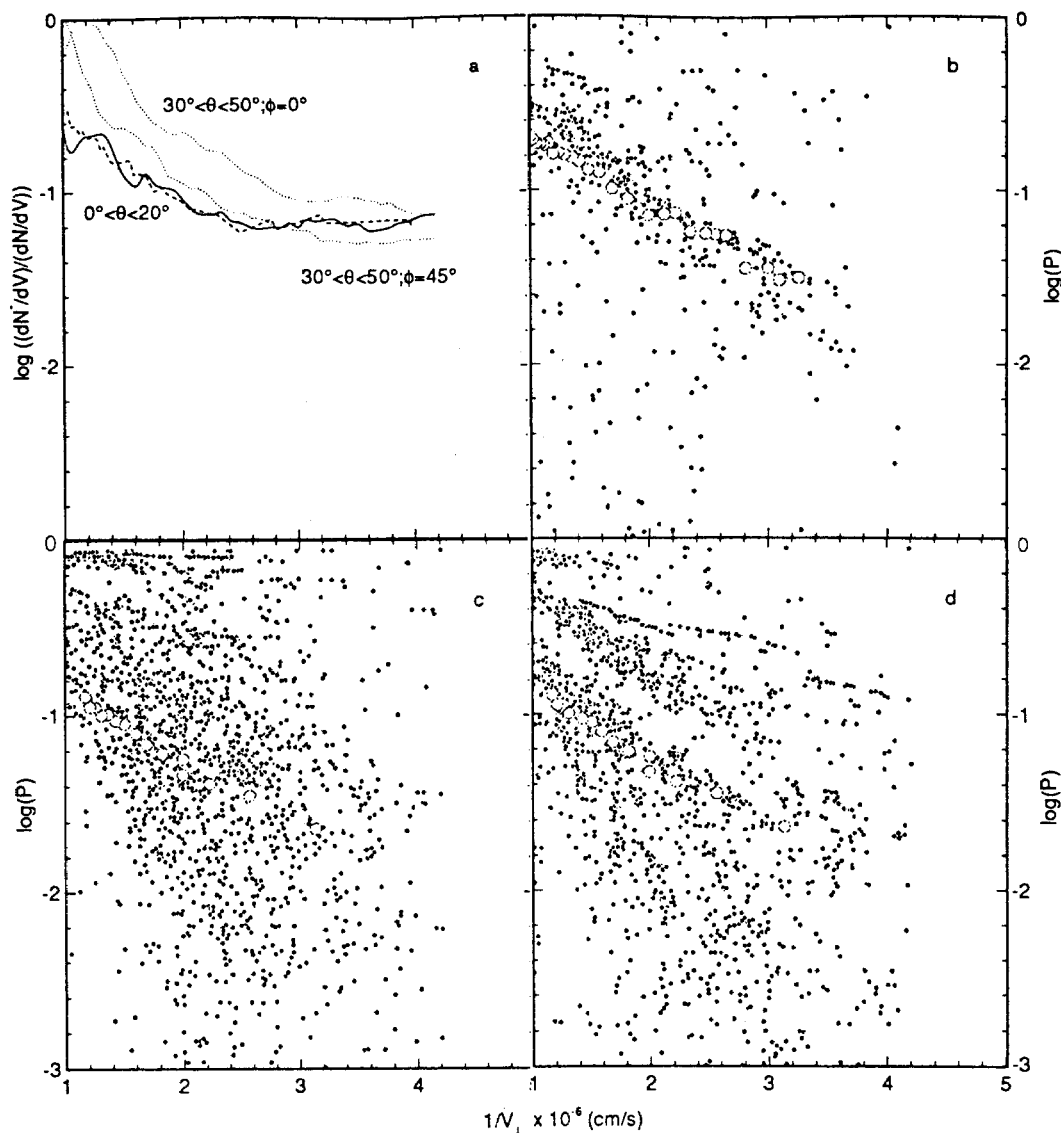


FIG. 4. Final excitation probabilities obtained from the full computer simulation. Values of  $P$  for individual atoms are shown as a function of  $1/v_{\perp}$ . Data for three different directions of ejection are shown. These are (b) normal to the surface ( $0^{\circ} < \theta < 20^{\circ}$ ), (c) along the open azimuthal direction ( $\varphi = 0^{\circ}$ ,  $30^{\circ} < \theta < 50^{\circ}$ ), and (d) along the close-packed azimuthal direction ( $\varphi = 45^{\circ}$ ,  $30^{\circ} < \theta < 50^{\circ}$ ). Frame (a) shows the averaged values for these normal (solid line) and off-normal (dotted lines) directions of ejection. Also shown in the same frame is the experimental data (dashed line) for normal ejection. In frame (b) the ideal case values for straight-up ejection are shown as open circles. In frames (c) and (d) the ideal case values for head-on ( $\theta_i = 45^{\circ}$ ) collisions are shown as open circles.

surface atom and is reexcited. At this point, the surrounding electron density is lower and the final excitation probability is consequently higher. These collisional processes can often be similar to those shown in Figs. 3(c) and 3(d) except that the collision with the neighboring atom is harder, i.e., the atom is moving faster. These types of collisions also occur for atoms that are directly hit by the primary particle (Ar in this case) which then reflect off a second layer atom and hit another first layer atom getting reexcited. The middle band ( $0.0225e^{-}/\text{\AA}^3 < \rho_i < 0.040e^{-}/\text{\AA}^3$ ) constitutes direct ejections following excitations in a disrupted environment, which has a lower density. For both the normal and off-normal cases, the bands below the ideal case line are, for the most part, what one would call typical ejection processes where an atom is hit from below and ejects into the vacuum.

The average ratio of the excited state intensity to the

ground state intensity is shown in Fig. 4(a) for these three angle ranges along with the experimental data for ejection normal to the surface. As with the height model, we find that the calculated values for ejection normal to the surface are very much in agreement with the experimental data. We also find that the calculated values in the high velocity regime for off-normal ejection are considerably larger than for ejection normal to the surface. In contrast, the experimental values are reasonably independent of angle for these angles of ejection.<sup>13</sup> This difference is due to the predominance of the reexcitation bands in the high velocity regions for the off-normal ejections, which tends to significantly raise the averages.

The curves shown in Fig. 4(a) exhibit a plateau in the low velocity regime in contrast to the ideal case values (Fig. 2). As discussed previously,<sup>13,14,18</sup> this is due to collisions

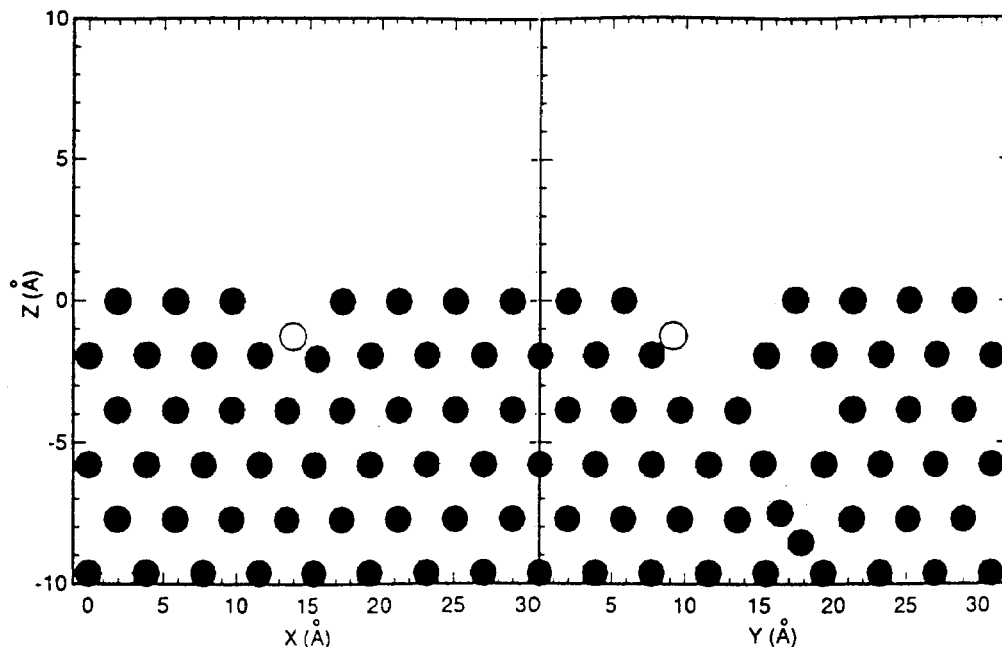


FIG. 5. Position snapshots of two perpendicular sections of the Rh crystal as an atom gets excited in a low-density environment below the surface. The atom (open circle) eventually ends up with a high excitation probability.

between ejecting atoms in the 1–20 Å region above the surface. These atoms are almost completely separated from the surface and little deexcitation occurs. In addition, this density model highlights the fact that some of the points at low velocity and high final excitation probability were actually excited at  $z < 0$  or below the original surface. Atom positions for such a collision sequence are shown in Fig. 5. The environment is not pristine. In fact, there is a small pit around the atom and the effective value of  $z$  that defines the surface is lower.

#### IV. CONCLUSIONS AND DIRECTIONS

An environment dependent quantity, the EAM density, has been used in a model designed to investigate the collisional details of the excitation–deexcitation process of excited Rh atoms ejected due to keV particle bombardment. The results from the model qualitatively reproduce the experimental data in which the ratio of the excited state intensity to ground state intensity of Rh atoms is exponentially dependent on the inverse of the perpendicular velocity at high velocities and is independent of velocity at low velocities. This treatment not only distinguishes surface excitations from those in the bulk, but also has the ability to distinguish between atoms that experience only slight differences in the environment. Using an environment dependent quantity like the EAM density, moreover, highlights the fact that simple idealized cases of the ejection process often fall far short of mimicking the real collisional events.

Although this model successfully explains many of the experimental details of the energy and angular distributions of Rh atoms ejected in fine-structure states, there is one major area of disagreement, thus affording the opportunity for further theoretical investigations. In particular, the average

calculated excitation probability in the high velocity region, especially in the off-normal directions, is much higher than the experimental value. The extra intensity in the calculated spectrum arises from the first two to three collisions, typically hard collisions, in the cascade. Specifically, the Ar hits one Rh atom which then reflects off the second layer and ejects. As discussed in Sec. III this target Rh atom may experience a second hard collision with one of its neighboring Rh atoms before ejecting. A consequence of the model presented here is that the electron density is very small and thus the instantaneous excitation probability is large. The reasons for the disagreement between the calculated and experimental results can revolve around either whether all the relevant physics has been included or whether the theoretical description is correct. On the experimental side, there are other higher lying excited fine-structure states. We have made no attempt to extract them in the calculations. Second, it is possible that the very hard collisions result in core excitations of the order of 200 eV as proposed by Shapiro and Tombrello.<sup>26</sup> They accounted for these excitations by removing the electronic excitation energy from the kinetic energy of the particles. The inclusion of this mechanism would undoubtedly reduce the calculated excitation probability for the fine-structure state in the high velocity regime.

Finally, it is appropriate to point out that some other dependency of the lifetime on the density in Eq. (3) might provide a better description of the nonradiative deexcitation process. In particular the density, and thus the lifetime, depend approximately exponentially on the height above the surface. Since the instantaneous excitation probability depends approximately exponentially on the lifetime, there is a very strong dependence of the final excitation probability on the height. There are some trajectories that appear very simi-

lar to each other including the value of the local density at the time of excitation yet result in quite different final excitation probabilities. One alternative relationship might be  $\tau = -\ln \rho$ .<sup>27</sup> At this point without a firmer theoretical foundation any attempts to use other expressions for the lifetime would be merely curve fitting.

The concept of using an environment dependent quantity to examine other electronic events such as ionization could be useful. For example, in clean metals the number of ions ejected can be  $10^5$  times or more smaller than the number of neutral atoms. It has been proposed that the ions could be ejected from a few rare trajectories in which a multitude of atoms eject (a megaevent).<sup>2,28</sup> The idea behind this proposal is that in these trajectories the particles are ejecting from a very disrupted environment and the final ionization probability is higher.

## ACKNOWLEDGMENTS

We gratefully acknowledge the financial support of the National Science Foundation. Penn State University supplied a generous grant of computer time. We also appreciate helpful discussions with Dan Bernardo and Nicholas Winograd.

<sup>1</sup>See, for example, N. Winograd and B. J. Garrison, in *Ion Spectroscopies for Surface Analysis*, edited by A. W. Czanderna and D. Hercules (Plenum, New York, 1991), pp. 45–141, and references therein.

<sup>2</sup>D. E. Harrison, Jr., *CRC Review in Solid State Materials Science*, edited by J. E. Greene (Chemical Rubber, Boca Raton, 1988), Vol. 14, p. S1.

- <sup>3</sup>J. K. Norskov, *Phys. Rev. B* **26**, 2875 (1982).  
<sup>4</sup>A. Blandin, A. Nourtier, and D. W. Hone, *J. Phys.* **37**, 396 (1976).  
<sup>5</sup>R. Brako and D. M. News, *Surf. Sci.* **108**, 253 (1981).  
<sup>6</sup>M. L. Yu and N. D. Lang, *Phys. Rev. Lett.* **50**, 127 (1983).  
<sup>7</sup>N. D. Lang, *Phys. Rev. B* **27**, 2019 (1983).  
<sup>8</sup>J. K. Norskov and B. I. Lundquist, *Phys. Rev. B* **19**, 5661 (1979).  
<sup>9</sup>A. Nourtier, J. P. Jardin, and J. Quazza, *Phys. Rev. B* **37**, 10,628 (1988).  
<sup>10</sup>Z. Sroubek, K. Zdansky, and J. Zavadil, *Phys. Rev. Lett.* **45**, 580 (1980).  
<sup>11</sup>J. H. Lin and B. J. Garrison, *J. Vac. Sci. Technol. A* **1**, 1205 (1983).  
<sup>12</sup>J. A. Olson and B. J. Garrison, *J. Chem. Phys.* **83**, 1392 (1985).  
<sup>13</sup>N. Winograd, M. El-Maazawi, R. Maboudian, Z. Postawa, D. N. Bernardo, and B. J. Garrison, *J. Chem. Phys.* **96**, 6314 (1992).  
<sup>14</sup>D. N. Bernardo, M. El-Maazawi, R. Maboudian, Z. Postawa, N. Winograd, and B. J. Garrison, *J. Chem. Phys.* **97**, 3846 (1992).  
<sup>15</sup>M. S. Daw and M. I. Baskes, *Phys. Rev. Lett.* **50**, 1285 (1983).  
<sup>16</sup>M. S. Daw and M. I. Baskes, *Phys. Rev. B* **29**, 6443 (1984).  
<sup>17</sup>S. M. Foiles, M. I. Baskes, and M. S. Daw, *Phys. Rev. B* **33**, 7983 (1986).  
<sup>18</sup>D. N. Bernardo, R. Bhatia, and B. J. Garrison, *Comput. Phys. Commun.* (in press).  
<sup>19</sup>M. H. Shapiro and J. Fine, *Nucl. Instrum. Methods B* **44**, 43 (1989).  
<sup>20</sup>J. J. Vrakking and A. Kroes, *Surf. Sci.* **84**, 153 (1979).  
<sup>21</sup>U. Fano and W. Lichten, *Phys. Rev. Lett.* **14**, 627 (1965).  
<sup>22</sup>H. D. Hagstrum, *Phys. Rev.* **96**, 336 (1954).  
<sup>23</sup>N. Mårtensson, R. Nyholm, and B. Johansson, *Phys. Rev. Lett.* **45**, 754 (1980).  
<sup>24</sup>P. Sigmund *et al.*, *Nucl. Instrum. Methods B* **36**, 110 (1989).  
<sup>25</sup>The erratum is in this issue. Basically the lifetime was a constant to a height of about 1.2 Å and then it was to increase exponentially to infinity. In effect, at the height of 1.2 Å it increased to infinity and thus terminated any deexcitation processes. There is some decay but not all that should be present.  
<sup>26</sup>M. H. Shapiro and T. A. Tombrello, *Nucl. Instrum. Methods B* (in press).  
<sup>27</sup>For the density used here the values of  $\rho$  do not get larger than 1.  
<sup>28</sup>P. Williams, *Surf. Sci.* **90**, 588 (1979).